



Computational analyses for tunable solid lenses coupling polyacrylamide hydrogel electrodes

HUI ZHANG* , MIN DAI, ZHIJIE XIA and ZHISHENG ZHANG

School of Mechanical Engineering, Southeast University, Nanjing 211189, China

*Author for correspondence (103200003@seu.edu.cn)

MS received 29 May 2020; accepted 22 October 2020

Abstract. Electrically tunable lenses could change focus without motor-controlled translations of stiff lenses. Firstly, the lens system is enabled by stable polyacrylamide (PAM) hydrogel electrodes that are synthesized containing silicone oil, sodium chloride, etc. Two layers of the hydrogel are used as ionic conductors to sandwich a dielectric elastomer membrane. The maximum rupture stretch of the hydrogel was around 20 and the small strain Young's modulus was about 0.5 kPa in experiments. Secondly, compact computational models are proposed based on the assumption of homogeneous deformation on materials, and the application of energy methods. Thickness-stretch curves of the PAM hydrogel are calculated, and the relation between electric field and stretch of a lens actuator is obtained by using the built mathematic models. Thirdly, a soft solid-body lens is described to obtain compact tunable results. The relationship between the applied voltage and the focus has also been given based on the derived equations. An increase in lens size produced larger tunable range variation. The new lens could find application in systems requiring large variations of focus with silent operation, low weight, shock tolerance, etc.

Keywords. Dielectric elastomer; solid-body lens; polyacrylamide hydrogel.

1. Introduction

To overcome the typical limitations in terms of size, weight, complexity and energy consumption of stiff lenses, optical tunable lenses including liquid-based or solid-body lens are developed without mechanical parts. The key factors of a tunable lens are high efficiency and repeatable adjustability in its focus. An adaptive soft lens is able to find application in portable electronics and machine vision [1,2]. However, it might be preferable to use an elastic solid-body lens rather than a liquid-based lens in the cases that are particularly sensitive to mechanical vibrations, temperature changes and distortions introduced by gravity.

Soft tunable lenses are usually fabricated by dielectric elastomers (DEs) coupling with soft electrodes. Existing soft electrodes include carbon grease, micro-cracked gold films [3], metallic wires, etc. Metal films are opaque and have relatively small stretch ability [4]. The opaqueness of the carbon grease limits the applications in tunable optics [5]. It is desirable to replace the traditional carbon grease with flexible and transparent electrodes in optical lenses. Many transparent hydrogels that are biocompatible are ideal to meet this requirement. Hydrogels, as a kind of ionic conductors, usually have low elastic modulus and high stretchability [4,6]. Their electro-chemical performance can be maintained under different mechanical

loading (e.g., compressing, bending or stretching), and this kind of conductors could achieve fast response and large strain [7,8].

2. Synthesis of hydrogel and theoretical analysis

Polyacrylamide (PAM) and sodium chloride (NaCl) powder were dissolved in water. The concentration of PAM was set to be 2.1%, and the concentration of NaCl was set to be 2–4%. Silicone oil was subsequently added into the mixed solution. The uniformly mixed solution was transferred into a plastic/glass mould with diameter d (30, 50, 80, 100 mm) \times h (0.2, 0.4, 0.6, 0.8 mm), and then gelled in air for about 1 h. The hydrogels are transparent and flexible as shown in figure 1a. The transparency of the hydrogels enables a lens placed in the path of light. The non-volatility enables the lens to be used in open air.

The elastic solid-body lens we propose relies on thin insulating membranes made of VHB 4910 (3 M) that is covered by PAM hydrogels to form soft capacitors that can be deformed by applied voltages. As in figure 1b, the DE membrane was fixed on a circular rigid plastic frame with diameter 10 cm. Two sheets of the hydrogel on VHB surfaces were linked to copper electrodes that were connected to a power source. No delamination between the hydrogel and the dielectric was observed during

experiments. The conductivity increased with the concentration of NaCl in experimental observation. When the hydrogel was stretched, the electrode film was more transparent.

Figure 2 illustrates the theoretical prediction of the stretch for the PAM hydrogel with different reference radius R (5, 10, 15 mm) and thicknesses H (0.2, 0.4, 0.6 mm). According to the formula: $p_{\text{pre}} = RHs_{\text{gel}}$, here the pressure

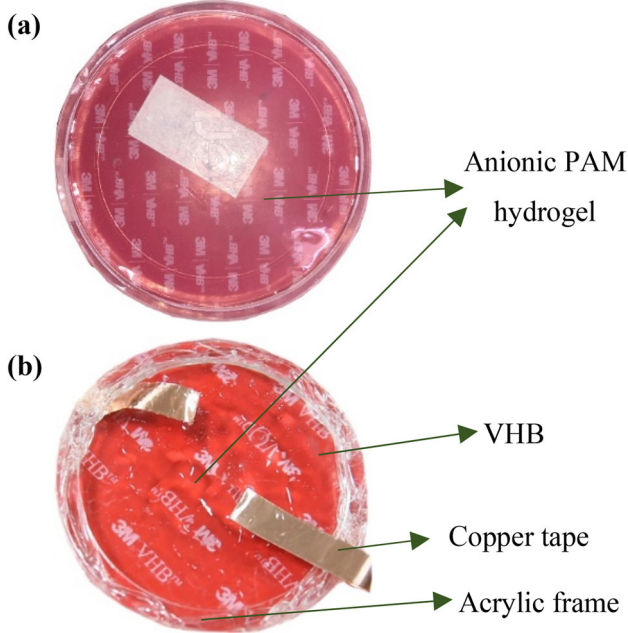


Figure 1. (a) The PAM hydrogel containing NaCl is highly transparent and flexible. (b) An actuator for a tunable lens that consists of a frame, a thin DE membrane (the pre-stretch $\lambda_p = 1$, the thickness $H = 0.5$ mm) with hydrogel electrodes.

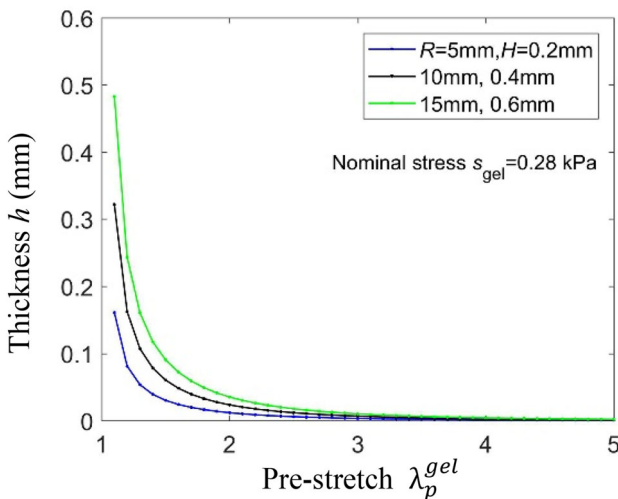


Figure 2. Theoretical prediction of the stretch using constant nominal stress for the PAM hydrogel with different original thicknesses and radii.

p_{pre} and the nominal stress s_{gel} are defined with respect to the pre-stretched state of the hydrogel [9]. Then exists,

$$\lambda_p^{\text{gel}} s_{\text{gel}} = \frac{\mu_{\text{gel}} \left[(\lambda_p^{\text{gel}})^2 - (\lambda_p^{\text{gel}})^{-4} \right]}{1 - \frac{2(\lambda_p^{\text{gel}})^2 + (\lambda_p^{\text{gel}})^{-4} - 3}{J_{\text{lim}}^{\text{gel}}}} \quad (1)$$

λ_p^{gel} is the pre-stretch of the hydrogel film. The parameters used in the simulation are: the shear modulus $\mu_{\text{gel}} = 0.6$ kPa, and the extension limit $J_{\text{lim}}^{\text{gel}} = 500$. The maximum rupture stretch of the hydrogel [10] is about 20, and the small strain Young's modulus is around 0.5 kPa in experiments. Although the loss of water from hydrogels could be an issue in some applications, the hydrogel electrodes were stable.

Figure 3 shows the schematic of a DEA for tunable lenses. In the reference state, a circular DE membrane, radius R and thickness H , is subject to no force and voltage. The radius of a circular hydrogel layer is $A\lambda_p$ as pre-stretched VHB membrane, and its thickness is $H_2/2$. In the pre-stretched state, the DE film is subject to an equi-biaxial pre-stretch, λ_p , and is attached to a circular rigid frame. The active region is pre-stretched to a circle of radius $A\lambda_p$, and then covered with two layers of the hydrogel with the same radius. The thickness of the DE film is $h_1 = H/\lambda_p^2$, and the combined thickness of the two hydrogel films is H_2 . In the actuated state, subject to a voltage, the thickness of the dielectric reduces to h and the radius of the active region becomes $A\lambda$.

The energy of the active region is attributed to the elastic energy of both DE and hydrogel, and the dielectric energy of DE [11]. The hydrogel also contributes to the total volume of the active region. The Gent model represents the active region energy of the DE and hydrogel with different shear modulus μ_i , and extension limit J_{lim}^i , where $i = \text{DE or gel}$. The energy density of the active region can be written as

$$W(\lambda, D) = \frac{h_1}{h_1 + H_2} W_{\text{DE}}(\lambda) + \left(1 - \frac{h_1}{h_1 + H_2}\right) W_{\text{gel}}(\lambda) + \frac{h_1}{h_1 + H_2} W_{\text{DE}}(\lambda, D) \quad (2)$$

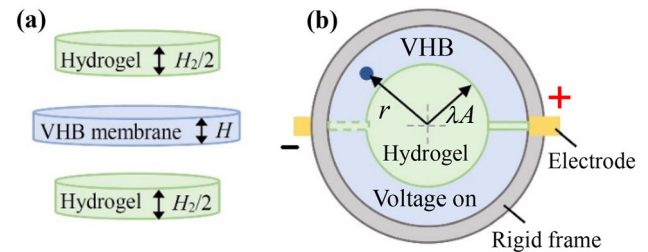


Figure 3. The schematic of an actuator made of a DE sandwiched between hydrogels. (a) In the reference state, a circular DE membrane with thickness H , the combined thickness of the two hydrogel films is H_2 . (b) In an actuated state, a material particle is marked by radius r that changes from reference R , and the radius of the active region moves to λA from reference A .

The nominal stress s , defined with respect to the state of the DE membrane, is evaluated namely

$$\lambda s = \lambda \frac{\partial W}{\partial \lambda} = \frac{\mu(\lambda^2 - \lambda^{-4})}{1 - \frac{2\lambda^2 + \lambda^{-4} - 3}{J_{lim}^{DE}}} \quad (3)$$

The average true stress is $\sigma = \frac{h_1}{h_1 + H_2} \lambda s$. Then the expression for the stress of active region at the actuated state, exists [12],

$$\begin{aligned} \sigma + \frac{h_1}{h_1 + H_2} \varepsilon E^2 &= \frac{h_1}{h_1 + H_2} \times \frac{\mu_{DE}(\lambda^2 - \lambda^{-4})}{1 - \frac{2\lambda^2 + \lambda^{-4} - 3}{J_{lim}^{DE}}} \\ &+ \left(1 - \frac{h_1}{h_1 + H_2}\right) \\ &\times \frac{\mu_{gel}(\lambda^2 \lambda_p^{-2} - \lambda^{-4} \lambda_p^4)}{1 - \frac{2\lambda^2 \lambda_p^{-2} + \lambda^{-4} \lambda_p^4 - 3}{J_{lim}^{gel}}} \end{aligned} \quad (4)$$

The parameters are used as: $\mu_{DE} = 20$ kPa, $J_{lim}^{DE} = 250$, the thicknesses $H = 0.5$ mm, $H_2 = 0.5$ mm, the pre-stretch $\lambda_p = 1$ or 2, and the relative permittivity of DE is set to be $\varepsilon = 4.161 \times 10^{-11}$ F m⁻¹. Figure 4 shows the voltage–stretch behaviour by using a theoretical model that accounts for the constraint of the hydrogels [8]. Subject to a voltage, the active part covered by the hydrogel expands with homogeneous deformation [13]. The electric field relates to the actuating voltage Φ , and $E = \lambda^2 \frac{\Phi}{H}$. Both thickness of the hydrogel and the pre-stretch of the dielectric affect voltage–stretch curves. Large actuated deformation is attainable under the conditions of large pre-stretch of DEs [14] and thin hydrogels.

3. Tunable solid-body lens and governing equations

When the deformed shape of a circular membrane is assumed to be a portion of a sphere, a DE actuator could be used to stimulate curvature changes of a tunable lens [15]. It is crucial to study the function between applied voltages and

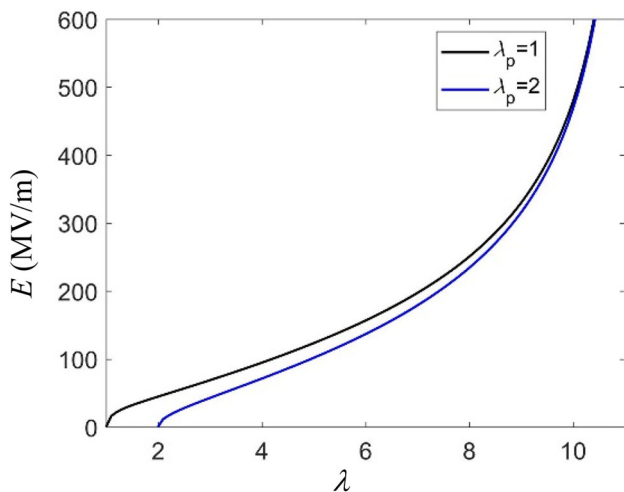


Figure 4. The predicted curves between electric field and stretch. Different levels of pre-stretches from $\lambda_p = 1$ to 2 were imposed to the DE actuator coupling the PAM hydrogel.

various focus in a solid-body lens coupling hydrogel electrodes, but most researchers just have given experimental observations to describe the relation. The focal length is adjustable by applying different voltages. The increased tuning range of a lens is mainly due to the high electric field that could be applied before breakdown of material.

According to mechanical force, the Gent model, the equations (2 and 4), the effective equation is obtained as follows:

$$\begin{aligned} \frac{h_1}{h_1 + H_2} \varepsilon E^2 &= \frac{h_1}{h_1 + H_2} \times \lambda \frac{\partial W_{DE}}{\partial \lambda} + \left(1 - \frac{h_1}{h_1 + H_2}\right) \\ &\times \lambda \frac{\partial W_{gel}}{\partial \lambda} \end{aligned} \quad (5)$$

When there is without preload ($\lambda_{pre} = 1$), then,

$$\begin{aligned} \frac{h_1}{h_1 + H_2} \varepsilon E^2 &= \frac{h_1}{h_1 + H_2} \times \frac{\mu_{DE}(\lambda^2 - \lambda^{-4})}{1 - \frac{2\lambda^2 + \lambda^{-4} - 3}{J_{lim}^{DE}}} \\ &+ \left(1 - \frac{h_1}{h_1 + H_2}\right) \times \frac{\mu_{gel}(\lambda^2 - \lambda^{-4})}{1 - \frac{2\lambda^2 + \lambda^{-4} - 3}{J_{lim}^{gel}}} \end{aligned} \quad (6)$$

As shown in figure 5, the green circular area in image 5a is transparent hydrogel films with radius A and thickness H_2 , and the surface area is $S_A = \pi A^2$. The blue ring area with radius B and thickness H is a DE membrane. In the pre-stretched state, the whole lens film is uniformly stretched and fixed on a rigid frame. Due to the stretching effect, the radius of the active region changes to a , while the radius of the DE membrane changes to b (figure 5b). In the resting

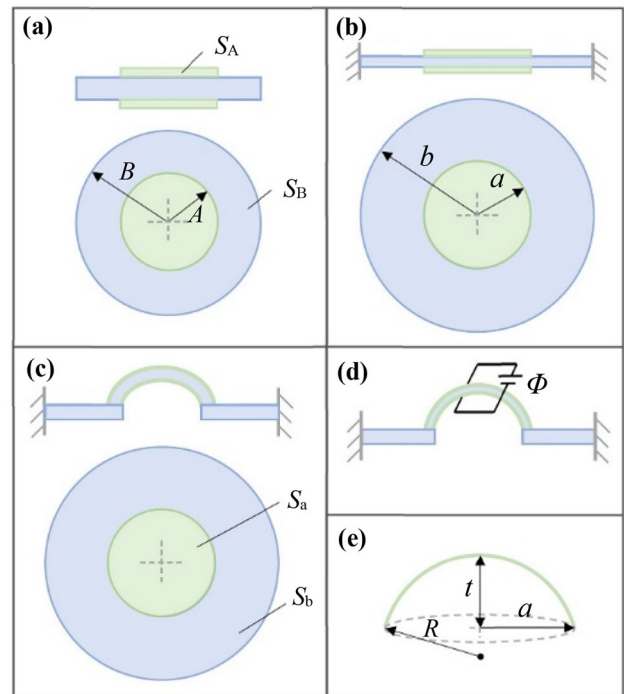


Figure 5. The deformation of a tunable solid-body lens. (a) Reference state. (b) Pre-stretched state. (c) Resting state. (d) Actuated state. (e) Representation of the lens as a spherical cap that has a cap height t , a base diameter $2a$, and the radius of curvature R .

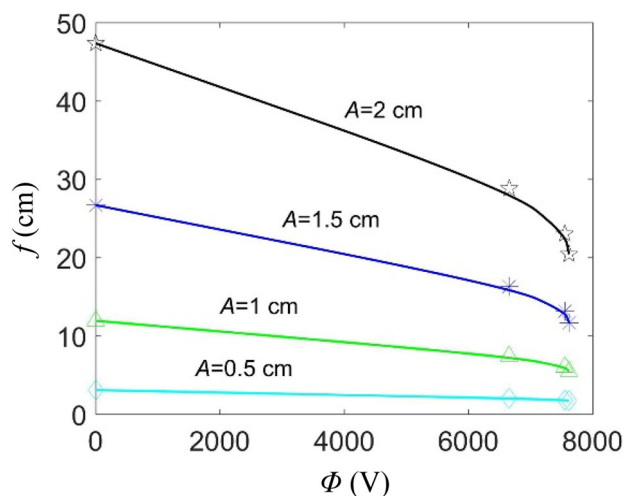


Figure 6. Variations of the lens focal length with the applied voltage.

state, the lens plane is compressed. In the actuated state, the shape of the lens is as a spherical cap with curvature radius R , and its projection is circular in the middle plane, whose radius is a [16]. The lens plane starts compressing and thinning by the electric field, and the radius of curvature is also reduced. Here t is the height between top of the cap and middle plane as shown in figure 5e.

From the geometrical relationship $a^2 + (R - t)^2 = R^2$, the radius of curvature can be written as $R = \frac{a^2 + t^2}{2t}$. The surface area of the spherical lens is:

$$S_a = 2\pi R^2 - [2\pi R \times (R - t)] \quad (7)$$

The optical properties of the lens are determined from its geometrical properties and the refractive index of its constitutive material. The effective focal length is computed using the general ‘thick-lens formula’, and the lens operates in air. R_1 and R_2 are the radii of two surface curvatures of the soft lens; n is the refractive index, and $n = 1.4235$. The lens thickness is much smaller than the radii of the curvatures. In addition, by considering that the lens is convex, so that $R_2 \rightarrow \infty$ and $R_1 = R$. Therefore, we get the equation $f = \frac{R}{n-1}$.

Figure 6 represents the focal-length variation in response to applied voltages for different original radius of the active area on the lens actuator (0.5, 1, 1.5 and 2 cm). As expected, an increase in lens size produces larger tunable range variation. This phenomenon is due to larger absolute expansions of the compliant hydrogel electrodes [17].

4. Conclusion

This article presents PAM hydrogel containing sodium chloride, this kind of transparent and stretchable hydrogel can function as soft conductors for optical lenses. The hydrogel electrodes possess high stabilities, including air, adhesion, non-corrosive and high voltage stability. By using the built

model, the thickness–stretch curves of the hydrogel conductor are calculated. Large actuated deformation is attainable under the conditions of large pre-stretch of DEs and thin hydrogels.

A configuration described is to obtain compact electrically tunable lenses entirely made of solid-body elastomers. As compared to DEA-based liquid lenses, this structure simplifies the fabrication process and allows for a higher versatility in design. Then the relation between lens focus and applied voltages is calculated. These effective mathematical formulas account for homogeneous deformation of the active region on lens surfaces. We expect the proposed models can provide some theoretical guidance for bionic lens designs.

Further development is needed to reduce the actuating voltage of the lens system. This type of adaptive lenses might find application in autofocus systems for portable consumer electronics, machine vision, etc.

Acknowledgement

This study was funded by National Natural Science Foundation of China (Grant Number 51775108), Natural Science Foundation of Jiangsu Province (Grant Number BK20190375).

References

- [1] Dai H, Zou J and Wang L 2016 *Appl. Phys. A* **122** 507
- [2] Pierce M C, Weigum S E, Jaslove J M, Richards-Kortum R and Tkaczyk T S 2014 *Ann. Biomed. Eng.* **42** 231
- [3] Rosset S and Shea H R 2013 *Appl. Phys. A* **110** 281
- [4] Shi L, Zhu Y X, Gao G X, Zhang X Y, Wei W, Liu W F *et al* 2018 *Nat. Commun.* **9** 2630
- [5] Shian S, Diebold R M and Clarke D R 2013 *Opt. Express* **21** 8669
- [6] Chen B H, Lu J J, Yang C H, Yang J H, Zhou J X, Chen Y M *et al* 2014 *Appl. Mater. Interfaces* **6** 7840
- [7] Keplinger C, Sun J Y, Foo C C, Rothemund P, Whitesides G and Suo Z G 2013 *Science* **341** 984
- [8] Chen B H, Bai Y Y, Xiang F, Sun J Y, Chen Y M, Wang H *et al* 2014 *J. Polym. Sci. B: Polym. Phys.* **52** 1055
- [9] Zhang H, Dai M and Zhang Z S 2019 *AIP Adv.* **9** 045010
- [10] Tang J D, Li T Y, Vlassak J J and Suo Z G 2016 *Soft Matter* **12** 1093
- [11] Godaba H, Zhang Z Q, Gupta U, Foo C C and Zhu J 2019 *Soft Matter* **15** 7137
- [12] Bozlar M, Punckt C, Korkut S, Zhu J, Foo C C, Suo Z G *et al* 2012 *Appl. Phys. Lett.* **101** 091907
- [13] Zhang H, Dai M and Zhang Z S 2019 *Optik* **178** 841
- [14] Fan P and Chen H 2018 *Appl. Phys. A* **124** 148
- [15] Jin B 2016 *Opt. Eng.* **55** 075101
- [16] Pieroni M, Lagomarsini C, Rossi D D and Carpi F 2016 *Bioinspir. Biomim.* **11** 065003
- [17] Wang Q, Cao Y J, Wang Y N, Liu J C and Xie Y X 2018 *Mech. Based Des. Struct.* **46** 800